We are IntechOpen, the world's leading publisher of Open Access books Built by scientists, for scientists

6,900
Open access books available

186,000
International authors and editors

200M
Downloads

Our authors are among the

154
Countries delivered to

TOP 1%
most cited scientists

12.2%
Contributors from top 500 universities

WEB OF SCIENCE™

Selection of our books indexed in the Book Citation Index in Web of Science™ Core Collection (BKCI)

Interested in publishing with us?
Contact book.department@intechopen.com

Numbers displayed above are based on latest data collected.
For more information visit www.intechopen.com

Chapter 2

Modeling and Control Strategy for Hybrid Electrical Vehicle

Vu Trieu Minh, Alina Sivitski, Mart Tamre and Igor Penkov

Additional information is available at the end of the chapter

http://dx.doi.org/10.5772/61415

Abstract

This chapter reviews the developments and configurations of hybrid electrical vehicles. A classic model for a parallel hybrid electrical vehicle is chosen and modeled. Model predictive controllers and simulations for this vehicle model are applied to control the vehicle speed and power to check the ability of the system to handle the transitional period for the automatic clutch engagement from the electrical driving to the internal combustion engine (ICE) driving. The chapter produces potential model predictive control considerations to achieve the optimal real-time control actions subject to the vehicle physical constraints. The new system can be applied for electronic control units in real hybrid vehicle powertrains.

Keywords: Model Predictive Control, Automatic Clutch Engagement, Hybrid Vehicle, Powertrain System

1. Introduction

Transportation accounts for more than 25% of the world energy demand and consumes more than 60% of the oil used each year. Transportation is completely relied by almost 95% on the petroleum products. Lack of fossil fuel supplies and the negative greenhouse effect on the environment have motivated automotive engineers to fabricate new car generations to cope the fuel consumption and emissions issues. Hybrid vehicles are now a new product of the automobile industry. Such vehicles are becoming more impressive as they are very efficient and reduce pollution. Hybrid vehicles offer a great improvement on the air quality emissions for vehicles that are empowered by gasoline.

Hybrid electric vehicles (HEVs) are the type of hybrid vehicles and electric vehicles which combine the best features of internal combustion engines (ICEs) and electric motors (EMs).

INTECH
open science | open minds

© 2015 The Author(s). Licensee InTech. This chapter is distributed under the terms of the Creative Commons Attribution License (http://creativecommons.org/licenses/by/3.0), which permits unrestricted use, distribution, and reproduction in any medium, provided the original work is properly cited.

Hybrid vehicles can perform with much less emission and can save 50% less fuel than the other new conventional vehicles in the same class. Modern hybrid vehicles can now recharge the electrical power from the regenerative braking process and store the electrical energy from the electrical plug-in at outdoor parking locations using renewable energy resources. Hybrid electrical vehicles can completely remove the idle emissions by shutting down the combustion engines and restart them when running.

There are many advantage reasons for using the combination of ICEs and EMs over ICEs alone: EMs can stop completely during the ICEs idle period. EMs can use much less energy than ICEs in low speed (less than 50 km/h) where most of vehicles have to operate in cities. While ICE vehicles can operate better only on the highways with high speed (above 50 km/h) since the ICEs achieve higher level of power-to weight ratio. Therefore, the main advantage of ICEs is on the higher power that can provide to vehicles. Then, the combination of ICEs and EMs can maintain the optimal operation in both low speed on busy roads and high speed on highways. The ICEs can automatically turn on and recharge the batteries for EMs when they get low.

A distinction of HEVs can be divided into two main types: the serial type and parallel types. In the serial type, the ICEs are not mechanically connected to the vehicle powertrain, but they are used only to run the electrical generator to supply the electrical power to batteries for EMs. The EMs now can use the electrical energy from their batteries to propel the vehicle. In the parallel type, both ICE and EM power sources are independently operated; therefore, they can both individually or commonly propel the vehicles. The most general configuration is that the ICE and EM are connected by an automatically controlled clutch. For the EM driving in low speeds, the clutch between the ICE and the EM is open and only the EM runs the vehicle. In high speeds, this clutch is closed and the ICE is started and propelled the vehicle while the EM is stopped off. At very high speeds or at critical heavy loads, this EM can be automatically activated on to support the ICE to drive the vehicle. To conclude, serial hybrids are less efficient and are more suitable for short-distance travel before exhausting their batteries. However parallel hybrids fuel consumption is greater than serial hybrids; gas/diesel engine has dominating role in parallel hybrids and thus battery pack can have less capacity. More information about parallel hybrids in the literature can be referred in [1, 2], and [3] references.

Initial approaches to switch the transition between EM and ICE power sources were drawn on heuristic information on the characteristics of ICEs vs EMs. In reference [4], rule-based was used and in reference [5], fuzzy logic was used as typical controlled schemes. A set of rules was applied to separate the requirements between the two power sources. These control plans were introduced in the early hybrid implementations. However [4] and [5] did not fully investigate the fuel use optimization. The dynamic engagements of the clutch between the ICE and the EM must be controlled as smooth as possible at the right time of engagement. For the safety and comfort reasons, the clutch engagement and the torque transmission are not permitted to cause any unacceptable acceleration or exceeded jerk. Several other control strategies for smothering the clutches engagement have been attempted including the back stepping control in reference [6], the optimal control in the reference [7], and the model predictive control in reference [8] to achieve faster and smoother clutches engagement between ICE and EM. In our research, a new predictive model for controlling the speeds of ICEs and

http://dx.doi.org/10.5772/61415

EMs is developed and applied to the engagement of the clutches, which can help to enhance the driving comfort and reduce the jerk on the parallel HEVs.

The main motivation of using the model predictive control (MPC) scheme in this chapter is the ability of the MPC to determine the optimization actions online in both linear and nonlinear systems. Model predictive control involves new mathematic algorithms that calculate an infinite sequence of input and output variables in order to optimize the future behavior of the systems. To date, MPC strategy can be found in many application areas including aerospace, automotive and petrochemical industries as referred in reference [9]. One of the advantages of MPC is its ability to cope with constraints from the open-loop optimal control problems. Achieving solution from the general constrained nonlinear models within an infinite prediction sequence becomes impractical because the numerical means to solve these problems can be only applied for a finite horizon length in order to obtain a real-time numerical solution. Therefore, only a finite moving horizon regulator can be considered in which the optimal problem is performed over a finite prediction sequence, and the prediction cost after the end of the horizon is estimated from a terminal penalty as shown in reference [10]. For ensuring the stability within a finite prediction length, most of the nonlinear model predictive control (NMPC) strategies have used a terminal constraints region at the end of the prediction length as indicated in references [11, 12], and [13]. Another NMPC method using a terminal constraints region named quasi-infinite horizon that guarantees the asymptotic closed-loop stability with the input constraints was developed in reference [14]. But then the nonlinear systems have both input constraints and output constraints, many difficulties will arise to satisfy the output constraints because of constraints imposed already in inputs. Therefore, another NMPC method without a terminal constraint region is developed in reference [15] using the softened output constraints. Further investigation on MPC such as robust model predictive control (RMPC) that guarantees stability in the existence of the model uncertainty using linear matrix inequalities (LMIs) subject to both input and output saturated constraints was developed in reference [16]. In this RMPC,the controller will soften the output constraints as penalty terms and add into its objective function. These terms will keep the output violation at low values until the constrained solution is returned.

If there are too many input and output constraints, the controller may not be able to provide the desired outputs because the MPC regulator is designed for always on-line implementation, any infeasible solution of the optimization problem cannot be allowed. In order to assure the system stability, the conventional MPC strategies usually want to delete or ignore some output constraints from its objective function. Deletion of some output constraints will make the system looser and then the probability that MPC can achieve an optimal solution will increase. Similarly, the robustness of MPC can also increase if some output setpoints can be relaxed and a new MPC scheme, which turns the constrained setpoints into constrained regions was developed in reference [17]. In our research, the robustness of MPC schemes is also examined with both deleting and changing the output constrained setpoints into constrained regions. In this case, the outputs violation can be regulated by changing the penalty values of the weighting items.

Coming next, we briefly present the characteristics of some typical HEV configurations. After that, one typical HEV configuration will be selected for developing its dynamic equations. Then, several MPC scheme are built to control the speeds of the ICEs and the EMs for each part of this HEV. Simulation and calculated examples are also provided after each section to illustrate our main ideas for each section. Finally, some conclusions are drawn and some suggestions for the future research are discussed.

2. HEVs configurations and reviews

The first concept of HEVs was initiated by Ferdinand Porsche at Lohner Coach Factory when he designed the "Mixte", a series hybrid vehicle based on his earlier electrical vehicle. This hybrid vehicle was installed with a gasoline ICE connected to an electrical generator and an EM propels the vehicle with a small battery for more reliability. This serial HEV concept grew until the late of 1960s. In 1972, Viktor Wouk developed his first prototype for parallel hybrid powertrain in General Motors namely "Godfather of the Hybrid". This turning point ignited the very fast growing progress in HEVs as we can see nowadays and branched in many different aspects such as regenerative braking issues, fuel consumption, emission, battery problems and so on. Worldwide sales of hybrid vehicles reached more than four (4) million units by December 2010 and sold over 80 countries and regions, led by the United States with more 2.5 million units. Regenerative braking, shutting down the engine at idle have reduced the fuel consumption and emissions. The main problem for HEVs now is relying on the cost and the weight of the large batteries and the starter/generator motors.

The recent technology of HEVs is the development of the diesel HEVs since diesel prices are cheaper than gasoline while diesels produce more energy, suffer less wear while operating at higher efficiency. Diesel ICE produces higher torque and offer longer mileage. Most diesel ICE can use 100% pure biodiesel and they don't need petroleum. Diesel ICEs are 20% to 40% more efficient and produce less carbon-dioxide emissions than gasoline ICEs. Diesels are widely popular in Europe, accounting for more than 50% of the car market there. If the diesel HEVs were in use, higher benefits from this system can be achieved.

2.1. Definitions

Conventional vehicles are propelled by only igniting fossil fuel in an ICE and converting the ignition energy into mechanical rotation and translation. In contrast, HEVs are characterized by using some combination of a primary propulsion unit (PPU) that can be fuel cell (FC) of an ICE or EM that can be either an electrochemical storage system such as a battery or an electrostatic super capacitor [22]. In addition to the above mentioned components, at least one electric motor is necessary in any HEV to help propel the vehicle either fully or partially. This combination of electric and fossil fuel energy, supervised with a high level controller called energy management strategy (EMS), can improve the performance of the vehicle from a fuel consumption and emission point of view. Comparing HEVs with conventional vehicles shows

http://dx.doi.org/10.5772/61415

that the former is more fuel efficient due to the engine operation optimization and the possibility of recovering the kinetic energy during braking [23].

EMs play the role of optimizing the efficiency of the ICE as well as energy recovery during braking. It can also use the excess power of the engine to charge the battery if the power demands on the final drive is lower than the power converted by the engine. Another role can be to assist the ICE in the cases that the ICE alone cannot fulfill the driver demands when the ICE is overloaded in some emergent cases.

There are basically four main advantages in hybridizing a conventional vehicle as follows:

1. Engine downsizing: When we use both EM and ICE in one single vehicle, it is possible to size the engine for the mean instead of the peak power demand. In such a way, the electrical buffer (EB) can compensate the lack of power in high power demand periods of driving via the EM. Hence, having a smaller ICE, the vehicle can be driven more efficiently in normal driving compared to having a larger ICE.

2. Regenerative braking possibility: The energy that is dissipated in conventional vehicles during braking can be regenerated and stored in the electric buffer using the electrical machine in its generator mode.

3. Pure electric drive: Having an EM together with the ICE has also advantages of letting the ICE shut down during the vehicle's low speeds in such a way that the controller shuts the ICE down and makes the EM propel the vehicle at low speed. This can also reduce both fuel consumption and emissions.

4. Improve control of the ICE: Since in HEVs, the propulsion power demand is a mix of power from the PPU and the EB, control of the ICE operating point, i.e., engine torque and speed, can be carried out with higher degree of freedom compared to a conventional vehicle and depending on which type of HEV we have. In addition, having an EM in the propulsion system responding to quick changes in propulsion power demand due to its smaller time constant compared to that of the ICE, gives the possibility to avoid transient ICE utilization.

Although HEVs have many advantages, they have some limitations as well. The first issue is the increased cost due to the presence of EMs, energy storage system, electrical converters, and so on. Safety issues due to existence of high voltage electricity and electromagnetic interference due to high frequency switching are also other problems to HEVs.

2.2. HEV configurations

As mentioned above, any HEV contains at least two sources of energy. These two sources can be coupled together in several different combinations according to the application. The most famous configurations are called series, parallel, series-parallel and heavy HEV [23]. The latter is though not a separate category but either a series or a parallel hybrid that is used in heavy delivery vehicles can run on gasoline or diesel. The following is a brief description of each configuration.

Series HEVs:

Series powertrain architecture is used in large vehicles such as locomotives and heavy duty trucks and not in passenger vehicles according to efficiency problems due to their component inefficiencies [24]. In this configuration, the ICE is not directly connected to the final transmission but via two electric machines. In such architecture, the engine mechanical output is first converted into electric energy using an electric generator and then this electric energy can either charge the battery when needed or bypass the buffer and propel the vehicle via a separate electric motor or a combination of these as is shown in Figure 1. Regenerative braking is also possible using the traction motor in generator mode and storing the electric energy into the buffer. So a series HEV needs three machines: one engine, one electric generator, and one electric traction motor.

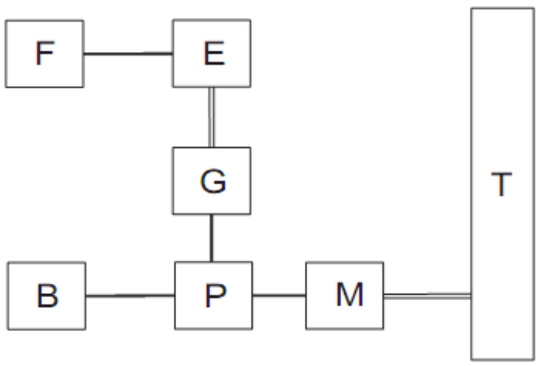

B: Battery; **E**: ICE; **F**: Fuel tank; **G**: Generator; **M**: Motor; **P**: Power converter; **T**: Transmission (including brakes, clutches and gears)

Figure 1. Series HEV Configuration.

Parallel HEVs:

Since the model that is used in this study is a parallel hybrid, it is described here in more details. In parallel hybrid electric vehicles the propulsion energy is delivered to the final drive by the EM and the ICE in two separate parallel paths. Though the ICE is the primary propulsion unit, the EM will be considered as an assistant to the PPU. As shown in Figure 2, both the ICE and the EM are coupled to the final transmission via mechanical links in parallel HEVs. Also, it is worth mentioning that each energy flow path can have a separate clutch to engage/disengage the final transmission from either the ICE and/or the EM. Hence, six (6) different operating modes are possible for a parallel HEV as follows:

1. Motor assist mode: Power from both the ICE and the EM are mixed together to provide the final drive power request. This can be the case in peak power demands. See Figure 3**A**.
2. Regenerative breaking mode: In this mode, the braking energy can be converted into electric energy, using the traction motor working in generator mode, and be stored into the electric buffer via the lower path. See Figure 3**B**.

http://dx.doi.org/10.5772/61415

3. Power split mode: This is the case when the ICE delivers more power than the power demand on final drive and the electric buffer is somehow empty (better say, its charge is close to its lower limit). So, ICE power is split in such a way that it drives the vehicle and the excess power charges the EB at the same time. In this mode, the electric machine works in generator mode. See Figure 3**C**.

4. Motor alone mode: In this mode, the ICE is turned off and the vehicle is fully powered by the EM. In this case, no fuel is used and hence there is no emission. This situation can happen mostly in idling or low power demand driving cases. See Figure 3**D**.

5. ICE alone mode: In ICE alone mode, the vehicle is propelled by the ICE and the EM is switched or via an electric circuit. See Figure 3**E**.

6. Stationary charging mode: In this mode, the vehicle is at standstill, all machineries are off and the vehicle is plugged into the power outlet.

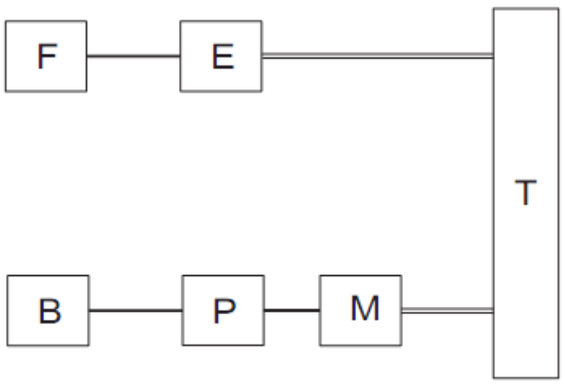

Figure 2. Parallel HEV configuration.

As can be seen in Figure 2, one single electric machine can be used in parallel HEVs, working either as a motor or as an electric generator. This results in a decrease in expenses as well as in total vehicle mass that can prevent an excess in fuel consumption due to the vehicle weight. Different operating modes of a parallel HEV are shown in Figure 3. Note that the arrowheads show the direction of power flow in each operating mode of the vehicle powertrains.

Series-parallel HEVs:

As shown in Figure 4, a third configuration of HEVs can be realized by just adding another power flow path to the parallel architecture having the features of both series and parallel HEV. In this configuration, an extra electric machine is added to the system via a mechanical and an electrical link so that all advantages of series and parallel hybrids can be kept together in one single vehicle. The disadvantage of series-parallel HEVs is though they have complex and costly structure, they are still preferred to be employed in some special cases.

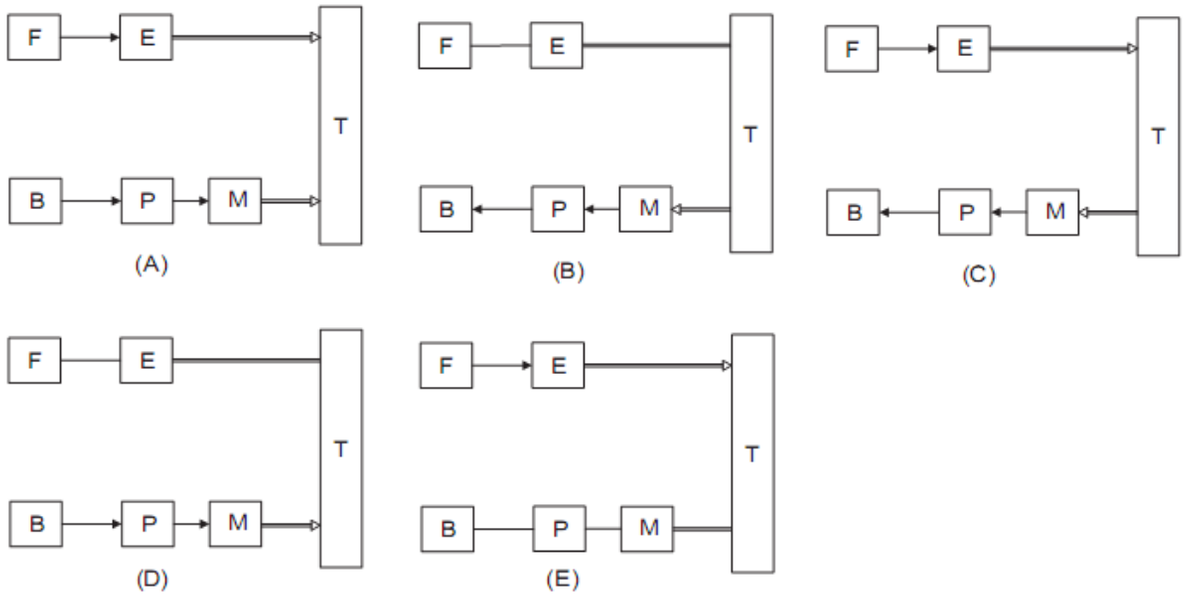

Figure 3. Power flow in a parallel HEV.

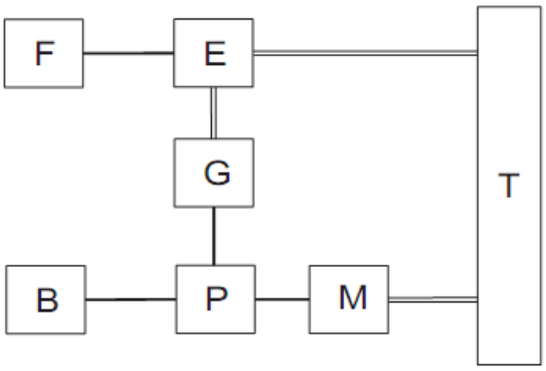

Figure 4. Series-parallel HEV.

2.3. Parallel HEVs reviews

There are four (4) different types of parallel hybrid vehicles: micro-hybrid, mild-hybrid, medium-hybrid, and full-hybrids. The differences are from their functionality relating to the electrical power and the input voltage level (Figure 5). Our research focuses only on the hybrid vehicle with light electrical power supplier up to approximately 10 kW. With these light electric power, some relatively high benefits can be obtained.

The input voltage for a mild-hybrid is usually applied at 36 V, but for this lightest electrical power, such a higher voltage level will not be needed and the 12 V will be a better solution. Due to the ability of some power assist for the regenerative braking, this configuration is categorized as mild-hybrid. The voltage level of medium-hybrid is 144 V while the voltage level for full-hybrid is 300 V. In this research, a full-hybrid vehicle is developed with two EMs.

http://dx.doi.org/10.5772/61415

One main EM uses the synchronous DC 300 V and the other is a synchronous starter/generator DC 48 V.

A conventional vehicle powertrain consists of one electrical starter connecting to one electrical generator. The electrical starter can convert the electrical energy into mechanical torque and is used to rotate the engine. The electrical generator is basically differing, it connects to the crankshaft and runs as an electrical supplier, transforming the ICE's mechanical torque into the electrical energy and stores this power into the vehicle batteries. The integrated starter generator (ISG) is a new development and becomes the only one device that will combine both above functions. For generating mode, it will charge the vehicle batteries and for starting mode, it will discharge the vehicle batteries in order to start or assist the ICE.

There are several possible positions for the ISG to be assembled. Three (3) main typically configurations are, the crankshaft-mounted ISG (C-ISG), the belt driven ISG (B-ISG), and the drivetrain mounted ISG (D-ISG) as shown from Figure 6 to Figure 8. The C- and D-ISG are usually used for the larger electrical power levels than the B-ISG configuration. Reasons for these differences are the limited power suppliers that can be transferred without slip through the belt of the B-ISG configuration. In the case of D-ISG configuration, the clutch is installed between the ICE and the ISG, so that, the hybrid vehicle can operate from either the ISG or on the combination of both power supplier sources. Rationally, if the vehicle can be able to operate completely on the ISG, the electrical power supplier must be large adequate.

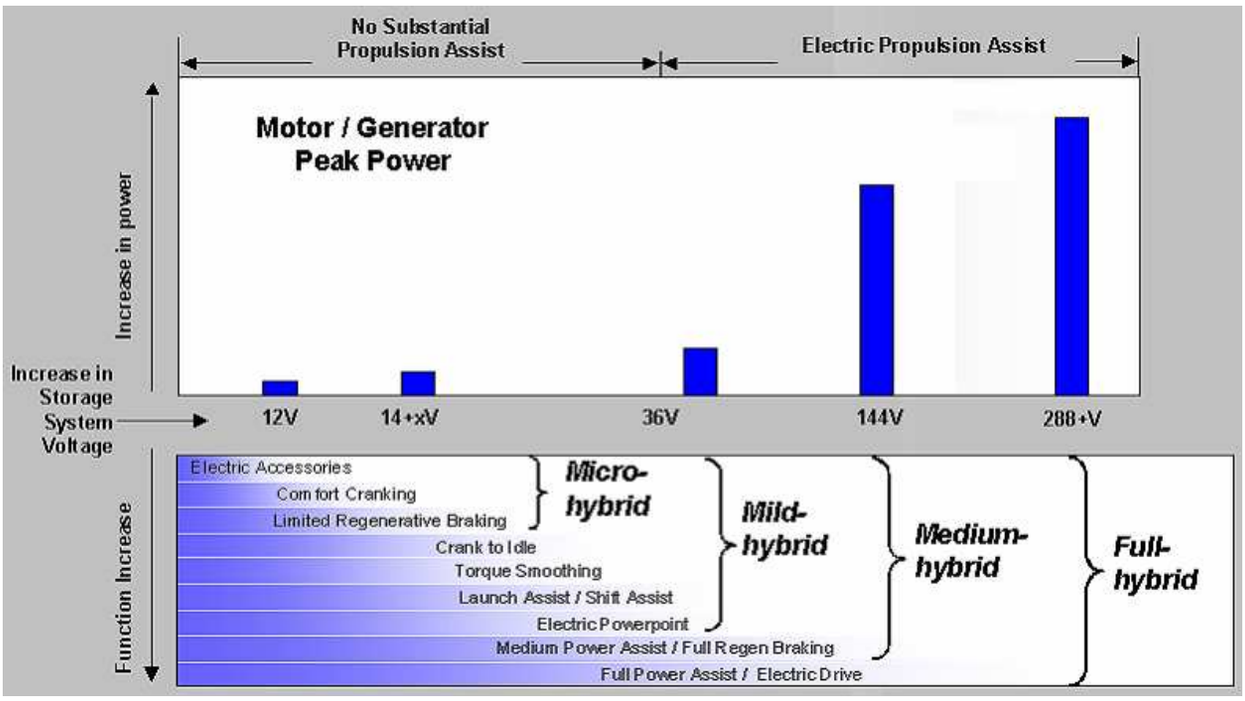

Figure 5. Different classes of hybridization [18].

One clear advantage of the D-ISG configuration regarding to other variants is that during deceleration the drag torque of the ICE can be removed by opening the clutch, letting more

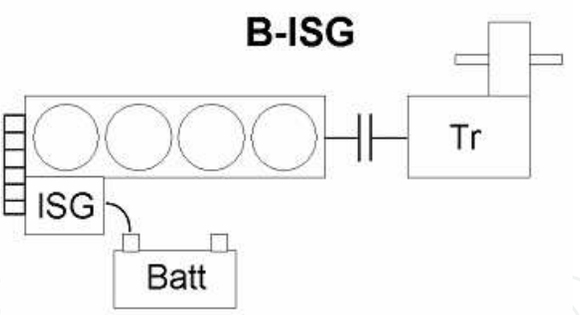

Figure 6. Schematic representation of a B-ISG.

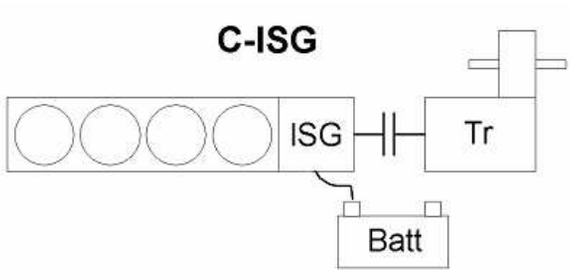

Figure 7. Schematic representation of a C-ISG.

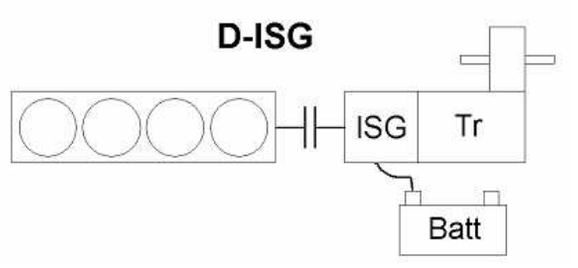

Figure 8. Schematic representation of a D-ISG.

energy available for regenerative braking processes. However, because of the limited charging acceptance of the vehicle batteries, the full ability of regenerative braking process will be never employed unless the deceleration is very slow. Additionally, purchasing a B-ISG system is less cost, which will provide some important advantages over the use of the C-ISG and the D-ISG.

From the above overview of HEV configurations, we will select a typical parallel HEV configuration and start the full investigation with this new HEV model in the next section.

3. HEV configuration and modeling

A typical update HEV for this research is shown in Figure 9. It is from a very common parallel HEV concept system designed by Daimler Chrysler, namely the P12-Configuration appeared

http://dx.doi.org/10.5772/61415

at the 2004 Detroit Motor Show. The model concept includes one (1) conventional ICE and two (2) EM1 and EM2. An automatically controllable conventional friction clutch separates the model drivetrain into two (2) parts: Part 1: ICE with EM1, and Part 2: EM2 and the rest of the powertrain transmission. The EM1 operates as an electrical starter and a supported electrical generator. No torque converter is installed in this configuration. The driven wheel of this model is the rear wheel, which is connected with a conventional automated transferred gearbox and a conventional differential gearbox.

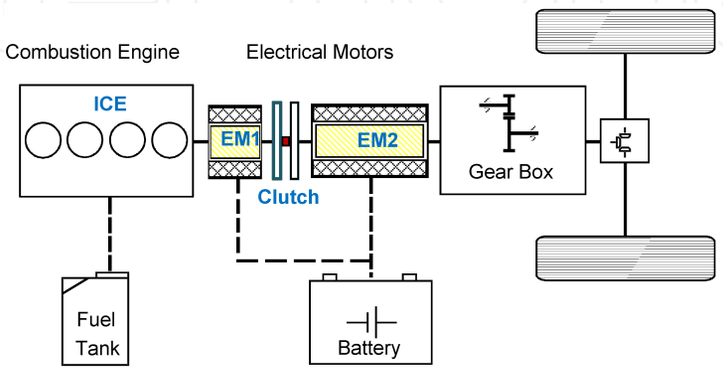

Figure 9. Configuration of the parallel hybrid powertrain.

At the only electrical driving for low speeds (below 50 km/h), the clutch between EM1 and EM2 is opened and the vehicle runs in a series hybrid configuration. For this operating mode, only second motor, EM2, drives the vehicle.

Transmission from the series mode to the parallel mode will be occurred at high speed (above 50 km/h) by closing the friction clutch between EM1 and EM2. EM1 will start the ICE for propelling the vehicle. After the ICE already started, the EM1 will turn off. EM2 will turn on if necessary as an electrical generator to charge the vehicle batteries.

In extreme heavy loads and from the control of the driver, both EM1 and EM2 can be simultaneously activated to assist the ICE to run the vehicle in critical driving conditions.

Our research concentrates on the development of reliable control strategies that can control the speeds of these two drivetrain parts and then, to synchronize these parts with a friction clutch to achieve the fast and smooth clutch engagement with reduction of driveline jerk and improvement of the driving comfort.

Figure 10 shows a simplified dynamic model for this hybrid transmission drivetrain. As referred in the references [19] and [20], the first part of the transmission powertrain can be approximately estimated by a lumped inertia of J_1 where the main shaft holding the ICE, EM1 and one friction clutch plate is modeled as a rigid frame. The second part of this transmission powertrain is also modeled by two inertias of J_2 and J_3 connected by a mechanical and damping springs. The conventional transmission gearbox and the differential gearbox are also modeled as a simple transforming torque with a variable term i depending on the selected gear transmission ratios.

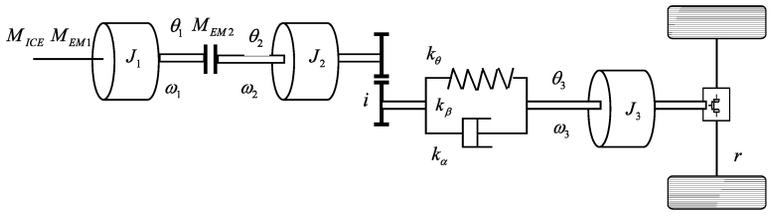

Figure 10. Simplified drivetrain structure.

where J_1 is the lumped inertia of ICE and EM1; J_2 is the inertia of EM2, and J_3 is the lumped inertia of the rest of the transmission powertrain. The transmission powertrain can now be considered as a connection of a spring with the torque stiffness k_θ, the velocity damping coefficient k_β, and the acceleration damping coefficient k_α. The torques are M_{ICE}, $M_{EM\,1}$, and $M_{EM\,2}$ generated from ICE, EM1, and EM2, respectively. Angular angles from shaft1, shaft2, and shaft3 are θ_1, θ_2, and θ_3. Angular velocities ω_1, ω_2, and ω_3 are measured from shaft1, shaft2, and shaft3 respectively. r is the vehicle wheel rolling radius.

There are three separated influences to the hybrid vehicle resistances by the air drag; the rolling friction resistance and the combined mechanical torque losses in the transmission gearbox; the differential gearbox and the shaft bearings due to friction. They can be approximately estimated from the hybrid vehicle velocity resistance torque, M_v, as:

$$M_v = \left(\frac{\rho}{2} c_w A (r\omega_3)^2 + f_r mg\right) r + a_0 + a_1\omega_3 + a_2\omega_3^2 \tag{1}$$

where drag coefficient; A: vehicle frontal area; ρ: air density; c_w; r: wheel dynamic radius; m: vehicle mass; f_r: resistance coefficient; a_i: polynomial coefficients; and g: natural gravity. The effect of the road dynamics and the road inclination can be considered as the additional disturbances to the system. These additional disturbances can cause some extra accelerating or decelerating torques at the rolling resistances. However, the changes of these effects and the changes of the vehicle load/mass during the vehicle running are not considered in our chapter.

At low speed (less 50 km/h), the powertrain torque model is formulated without the contribution of the exponential term of ω_3^2 to M_v. And the linearization of the resistance torque M_v in the above equation (1) is now calculated as:

$$M_v = M_{v0} + k_v\omega_3 \tag{2}$$

where M_{v0} is the initial constant value for the air drag and k_v is the linear air drag coefficient. Because of the differences in gearbox ratios, the coefficient constant M_{v0} and k_v can be varied for each gearbox ratio.

http://dx.doi.org/10.5772/61415

The following torque equations are formulated for the first powertrain part:

$$M_{1o} = J_1 \dot{\omega}_1 \tag{3}$$

The driving torque is computed as:

$$M_{1o} = M_{ICE} + M_{M1} - M_C \tag{4}$$

The friction torque M_C transmitted by the clutch can be divided into two engagement modes:

The locked mode when the friction torque (M_C) exceeds the static friction capacity ($M_{f\max}^{Static}$):

$$M_C = \frac{2}{3} r_C F_{NC} \mu_S \text{ when } \left(M_C = M_{f\max}^{Static} \right) \tag{5}$$

where F_{NC}: normal force exerted on the clutch; r_C: clutch corresponding radius; and μ_S: clutch static friction coefficient.

And the slipping mode:

$$M_C = r_C F_{NC} sign(\omega_1 - \omega_2) \mu_K \text{ when } (M_C < M_{f\max}^{Static})$$

where μ_K: clutch slipping kinetic friction coefficient.

The following torque equations are applied for the second part:

$$\begin{aligned} &M_{2o} = k_\theta \theta_2 + \frac{k_\theta}{i} \theta_3 + k_v \omega_3 \qquad \text{a} \\ &\text{or} \\ &M_{2o} = J_2 \dot{\omega}_2 i + J_3 \dot{\omega}_3 + k_v \omega_3 \qquad \text{b} \end{aligned} \tag{6}$$

And

$$\dot{M}_{2o} = J_2 \ddot{\omega}_2 i + k_\alpha \left(\frac{\dot{\omega}_2}{i} - \dot{\omega}_3 \right) + k_\beta \left(\frac{\omega_2}{i} - \omega_3 \right) \tag{7}$$

The torque M_{2o} is computed:

$$M_{2o} = \left(M_{EM2} + M_c\right)\eta i - M_{v0} \tag{8}$$

with η: efficiency of gearbox and differential.

The above torque equations can be transformed to the following dynamic equations:

$$\dot{\theta}_1 = \omega_1 \tag{9}$$

$$\dot{\omega}_1 = -\frac{k_{\beta 1}\omega_1}{J_1} + \frac{M_{ICE}}{J_1} + \frac{M_{M1}}{J_1} + \frac{-M_C}{J_1} \tag{10}$$

where $k_{\beta 1}$ is friction coefficient in shaft 1.

$$\dot{\theta}_2 = \omega_2 \tag{11}$$

$$\dot{\omega}_2 = -\frac{k_{\beta 2}\omega_3}{J_2 i} - \frac{J_3\dot{\omega}_3}{J_2 i} - \frac{\eta M_{M2}}{J_2} + \frac{\eta M_C}{J_2} - \frac{M_{v0}}{J_2 i} \tag{12}$$

where $k_{\beta 2}$ is friction coefficient in shaft 2.

$$\dot{\theta}_3 = \omega_3 \tag{13}$$

$$\dot{\omega}_3 = \frac{k_{\beta 3}\omega_3}{J_3} + M_{v0} \tag{14}$$

where $k_{\beta 3}$ is friction coefficient in shaft 3.

$$\ddot{\omega}_3 = \frac{k_{\beta 2}\omega_2}{J_3 i} - \frac{(k_{\beta 2}J_2 i^2 + k_\alpha k_v)\omega_3}{J_2 J_3 i^2} - \left(\frac{k_v + k_\alpha}{J_3} + \frac{k_\alpha}{J_2 i^2}\right)\dot{\omega}_3 + \frac{k_\alpha \eta (M_{M2} + M_C)}{J_2 J_3 i} - \frac{k_\alpha M_{v0}}{J_2 J_3 i^2} \tag{15}$$

Replace the torque generated by a DC motor in the following formula:

$$M_{DC\_MOTOR} = \frac{k_T}{R_I}V - \frac{k_E k_T}{R_I}\omega \tag{16}$$

http://dx.doi.org/10.5772/61415

where M_{DC_MOTOR}: torque by DC Motor; k_T: motor torque constant, $k_T = \frac{M_{Torque}}{I_{Current}}$ (Nm/A); k_E: motor electromotive force (EMF) constant (V/ (rad/s)), $k_E = k_T$; R_I: terminal resistance (Ohm), V: power supply (Volts), and ω: angular velocity (rpm).

Then a new set of vehicle dynamics is installed as:

$$\dot{\theta}_1 = \begin{bmatrix} 0 + & \omega_1 + & 0 + & 0 + & 0 + & 0 + & 0 \end{bmatrix} + \begin{bmatrix} 0 + & 0 + & 0 + & 0 + & 0 \end{bmatrix} \tag{17}$$

$$\dot{\omega}_1 = \begin{bmatrix} 0 + & \dfrac{-\left(k_{\beta 1} + \dfrac{k_{E1}k_{T1}}{R_{I1}}\right)\omega_1}{J_1} + & 0 + & 0 + & 0 + & 0 + & 0 \end{bmatrix} + \begin{bmatrix} \dfrac{M_{ICE}}{J_1} + & \dfrac{k_{T1}V_1}{R_{I1}J_1} + & 0 + & \dfrac{-M_C}{J_1} + & 0 \end{bmatrix} \tag{18}$$

$$\dot{\theta}_2 = \begin{bmatrix} 0 + & 0 + & 0 + & \omega_2 + & 0 + & 0 + & 0 \end{bmatrix} + \begin{bmatrix} 0 + & 0 + & 0 + & 0 + & 0 + \end{bmatrix} \tag{19}$$

$$\begin{aligned} \dot{\omega}_2 = & \begin{bmatrix} 0 + & 0 + & 0 + & 0 + & 0 + & \dfrac{-\left(k_{\beta 2} + \dfrac{k_{E2}k_{T2}}{R_{I2}}\right)\omega_3}{J_2 i} + & \dfrac{-J_3\dot{\omega}_3}{J_2 i} \end{bmatrix} \\ & + \begin{bmatrix} 0 + & 0 + & \dfrac{-\eta k_{T2}V_2}{R_{I2}J_2} + & \dfrac{\eta M_C}{J_2} + & \dfrac{-M_{v0}}{J_2 i} \end{bmatrix} \end{aligned} \tag{20}$$

$$\dot{\theta}_3 = \begin{bmatrix} 0 + & 0 + & 0 + & 0 + & 0 + & \omega_3 + & 0 \end{bmatrix} + \begin{bmatrix} 0 + & 0 + & 0 + & 0 + & 0 \end{bmatrix} \tag{21}$$

$$\dot{\omega}_3 = \begin{bmatrix} 0 + & 0 + & 0 + & 0 + & 0 + & \dfrac{k_{\beta 3}\omega_3}{J_3} + & 0 \end{bmatrix} + \begin{bmatrix} 0 + & 0 + & 0 + & 0 + & M_{v0} \end{bmatrix} \tag{22}$$

$$\begin{aligned} \ddot{\omega}_3 = & \begin{bmatrix} 0 + & 0 + & 0 + & \dfrac{-\left(k_{\beta 2} + \dfrac{k_{E2}k_{T2}}{R_{I2}}\right)\omega_2}{J_3 i} + & 0 + & \dfrac{-\left(k_{\beta 2}J_2 i^2 + k_\alpha k_v\right)\omega_3}{J_2 J_3 i^2} + & -\left(\dfrac{k_v + k_\alpha}{J_3} + \dfrac{k_\alpha}{J_2 i^2}\right)\dot{\omega}_3 \end{bmatrix} \\ & + \begin{bmatrix} 0 + & 0 + & \dfrac{-k_\alpha \eta k_{T2}V_2}{R_{I2}J_2 J_3 i} + & \dfrac{k_\alpha \eta M_C}{J_2 J_3 i} + & \dfrac{-k_\alpha M_{v0}}{J_2 J_3 i^2} \end{bmatrix} \end{aligned} \tag{23}$$

If we define the state variables as $x_0=[\theta_1 \quad \omega_1 \quad \theta_2 \quad \omega_2 \quad \theta_2 \quad \omega_3 \quad \dot{\omega}_3]'$ for the positions, angular velocities, and acceleration on vehicle shafts 1, 2, 3 respectively, and the input variables as $u_0=[M_{ICE} \quad V_1 \quad V_2 \quad M_C \quad M_{v0}]'$ for the torque for ICE, voltage for EM1; voltage for EM2, torque on clutch, and the initial air-drag torque load, a space state form of the vehicle dynamics is set up:

$$\dot{x}_0 = \begin{bmatrix} 0 & 1 & 0 & 0 & 0 & 0 & 0 \\ 0 & \dfrac{-\left(k_{\beta 1}+\dfrac{k_{E1}k_{T1}}{R_1}\right)}{J_1} & 0 & 0 & 0 & 0 & 0 \\ 0 & 0 & 0 & 1 & 0 & 0 & 0 \\ 0 & 0 & 0 & 0 & 0 & \dfrac{-\left(k_{\beta 2}+\dfrac{k_{E2}k_{T2}}{R_2}\right)}{J_2 i} & \dfrac{-J_3\dot{\omega}_3}{J_2 i} \\ 0 & 0 & 0 & 0 & 0 & 1 & 0 \\ 0 & 0 & 0 & 0 & 0 & \dfrac{k_{\beta 3}\omega_3}{J_3} & 0 \\ 0 & 0 & 0 & \dfrac{-\left(k_{\beta 2}+\dfrac{k_{E2}k_{T2}}{R_2}\right)}{J_3 i} & 0 & \dfrac{-\left(k_{\beta 2}J_2 i^2+k_\alpha k_v\right)}{J_2 J_3 i^2} & -\left(\dfrac{k_v+k_\alpha}{J_3}+\dfrac{k_\alpha}{J_2 i^2}\right) \end{bmatrix} x_0 \\ + \begin{bmatrix} 0 & 0 & 0 & 0 & 0 \\ \dfrac{1}{J_1} & \dfrac{k_{T1}}{R_1 J_1} & 0 & \dfrac{-1}{J_1} & 0 \\ 0 & 0 & 0 & 0 & 0 \\ 0 & 0 & \dfrac{\eta k_{T2}}{R_2 J_2} & \dfrac{\eta}{J_2} & \dfrac{-1}{J_2 i} \\ 0 & 0 & 0 & 0 & 0 \\ 0 & 0 & 0 & 0 & 1 \\ 0 & 0 & \dfrac{k_\alpha \eta k_{T2}}{R_2 J_2 J_3 i} & \dfrac{k_\alpha \eta}{J_2 J_3 i} & \dfrac{-k_\alpha}{J_2 J_3 i^2} \end{bmatrix} u_0 \qquad (24)$$

The new dynamic modeling in (24) allows having a deep viewing on the acceleration $\dot{\omega}_3$ and jerk $\ddot{\omega}_3$ of HEVs. This is also one of the mail contributions of this study.

When the vehicle travels in low speed (below 50 km/h), only EM2 is running. Then, the inputs: $M_{ICE}=0$, $V_1=0$, $M_C=0$ and the state variables: $\theta_1=0$, $\omega_1=0$, the system becomes:

http://dx.doi.org/10.5772/61415

$$\begin{cases} \dot{x}_p = A_p x_p + B_p u_p \\ y_p = C_p x_p + D_p u_p \end{cases} \text{ with}$$

$$A_p = \begin{bmatrix} 0 & 1 & 0 & 0 \\ 0 & -\dfrac{k_{\beta 2} + \dfrac{k_{E2} k_{T2}}{R_{I2}}}{J_2} & 0 & 0 \\ 0 & 0 & 0 & 1 \\ 0 & 0 & 0 & -\dfrac{\left(k_{\beta 3} - k_v\right)}{J_3} \end{bmatrix}, B_p = \begin{bmatrix} 0 & 0 \\ \dfrac{k_{T2}}{R_{I2} J_2} & 0 \\ 0 & 0 \\ 0 & -1 \end{bmatrix} \tag{25}$$

$$C_p = \begin{bmatrix} 0 & 0 & 0 & 1 \\ k_\theta & 0 & \dfrac{k_\theta}{i} & 0 \end{bmatrix}; D_p = \begin{bmatrix} 0 & 0 \\ 0 & 1 \end{bmatrix}$$

where x_p=[θ_2 ω_2 θ_3 ω_3]', u_p=[V_2 M_{v0}]', the outputs, y_p=[ω_3 $T_{Torque3}$]', are the vehicle velocity (measured) ω_3 and the vehicle torque (unmeasured) $T_{Torque3}$ generated on shaft 3. In this case, the torsional rigidity (Torque/angle): $k_\theta = \dfrac{M_{Torque}}{\varphi} = \dfrac{GJ}{l}$, where φ is the angle of twist $\varphi = \theta_2 - \dfrac{\theta_3}{i}$ (rad). G is the shear modulus or modulus of rigidity of mild carbon steel, G=81500.10^6 (N/m). l is the length of the shaft where the torque is being applied, in this case, we assumed: l=1.5 (m) for the vehicle drivetrain length. J is the moment of inertia, $J = J_2 + J_3$ (m^4).

At the high speed (more than 50 km/h), EM1 starts ICE while the clutch is still open, the dynamic equations in the first part become:

$$\dot{\theta}_1 = \begin{bmatrix} 0 + & \omega_1 \end{bmatrix} + \begin{bmatrix} 0 + & 0 \end{bmatrix} \tag{26}$$

$$\dot{\omega}_1 = \begin{bmatrix} 0 & -\dfrac{\left(k_{\beta 1} + \dfrac{k_{E1} k_{T1}}{R_{I1}}\right)}{J_1} \omega_1 \end{bmatrix} + \begin{bmatrix} \dfrac{\varsigma k_{T1}}{R_{I1} J_1} V_1 + & \dfrac{1}{J_1} M_{ICE} \end{bmatrix} \tag{27}$$

where ς is a new coefficient added to the EM1 as a compensated load to the starting period.

Then the system becomes:

$$\begin{cases} \dot{x}_e = A_e x_e + B_e u_e \\ y_e = C_e x_e + D_e u_e \end{cases}, \text{ with}$$

$$A_s = \begin{bmatrix} 0 & 1 \\ 0 & -\dfrac{\left(k_{\beta 1} + \dfrac{k_{T1}^2}{R_{I1}}\right)}{J_1} \end{bmatrix}; B_s = \begin{bmatrix} 0 & 0 \\ \dfrac{\varsigma k_{T1}}{R_{I1} J_1} & \dfrac{1}{J_1} \end{bmatrix}$$

$$C_s = \begin{bmatrix} 0 & 1 \\ 0 & \dfrac{\left(k_{\beta 1} + \dfrac{k_{E1} k_{T1}}{R_1}\right)}{J_1} \end{bmatrix}; D_s = \begin{bmatrix} 0 & 0 \\ 0 & 0 \end{bmatrix} \tag{28}$$

where, $x_e=[\theta_1 \quad \omega_1]'$, $u_e=[V_1 \quad M_{ICE}]'$, $y_e=[\omega_1 \quad T_{Torque1}]'$. $T_{Torque1}$ is the output torque (unmeasured) on shaft 1.

Using comprehensive HEV modeling equations from (24) to (28), we can develop MPC controllers to this HEV in the next section.

4. Model predictive controller design

MPC is one of the advanced control theories that have been studied extensively by the research community. MPC provides the optimal solutions for the open-loop manipulated input trajectory that minimizes the difference between the predicted plant behavior and the desired plant behavior. MPC diverges from other control techniques in that the optimal control problem is solved on-line for the current state of the plant, rather than off-line as a feedback control policy. MPC has been broadly used in industries because of its ability to deal with the input and output constraints in the optimal control problems.

The success of model predictive control is greatly depending on the exactness in the open-loop horizon predictions, which in turn rely on the exactness of the plant models. Several issues about MPC still remain open and are of interest to researchers due to the lack of a theoretical basis such as offset-free properties and robustness of MPC toward the environment disturbances. In this research, we study the ability of MPC controllers for the HEVs subject to input and output constraints.

In this research, the duties of MPC are applied to control the output torques generated and transferred among the components and the velocities of each shafts for achieving smoother clutch engagements and higher driving comfort. The RMPC schemes for uncertain systems subject to input and output saturated constraints are referred to the reference in [16]. The predictive control with soften output constraints is referred to the reference in [17] when a new MPC controller with output regions is developed to improve the robustness of the controller for handling input and output constraints and rejecting disturbances. NMPC conditions for

http://dx.doi.org/10.5772/61415

stability with soften output constraints are referred to in reference [15]. Development of fault detection for control system using MPC is referred to in reference [21] where the MPC schemes can be reconfigured as the real-time for detecting faults to maintain the error free for the system. Some other newer strategies of HEVs and MPC are referred to in references [25, 26], and [27].

The formula in (24) can now be discretized into the following format:

$$\begin{cases} x_{t+1} = Ax_t + Bu_t \\ y_t = Cx_t + Du_t \end{cases}, \tag{29}$$

where x_t, u_t, and y_t are state variables, inputs and outputs, respectively; A, B, C, and C are static matrices.

The above system is subject to the following input and output constraints:

$$u_t \in \mathcal{U}, \Delta u_t = u_t - u_{t-1} \in \Delta\mathcal{U}, \text{ and } y_t \in \mathcal{Y} \tag{30}$$

The optimal problem for this MPC controller tracking some output setpoints can be presented in the following objective function:

$$\begin{aligned} &\min_{U \triangleq \left\{\Delta u_1, \ldots, \Delta u_{1+N_u-1}\right\}} \left\{ J(U, x(t)) = \sum_{k=0}^{N_y-1} \left[(y_{t+k|t} - r)' Q (y_{t+k|t} - r) + \Delta u'_{t+k} R \Delta u_{t+k} \right] \right\}, \\ &\text{subject to}: u_{t+k} \in \left[u_{\min}, u_{\max} \right], \Delta u_{t+k} \in \left[\Delta u_{\min}, \Delta u_{\max} \right], \text{ for } k = 0,1,\ldots,N_u - 1 \\ &y_{t+k|t} \in \left[y_{\min}, y_{\max} \right], \text{ for } k = 0,1,\ldots,N_y - 1 \\ &\Delta u_{t+k} = 0, \text{ for } k = 0,1,\ldots,N_y - 1 \\ &x_{t|t} = x(t), x_{t+k+1|t} = Ax_{t+k|t} + Bu_{t+k}, u_{t+k|t} = u_{t+k-1|t} + \Delta u_{t+k|t}, y_{t+k|t} = Cx_{t+k|t} + Du_{t+k|t} \end{aligned} \tag{31}$$

is solved at each time t, where $x_{t+k|t}$ denotes the predicted state vector at time $t+k$, obtained by applying the input increment sequence, $U \triangleq \{\Delta u_t, \ldots, \Delta u_{t+N_u-1}\}$, and the new inputs, $u_{t+k|t} = u_{t+k-1|t} + \Delta u_{t+k|t}$, to the model equation (29) starting from the state $x_t = x(t)$. $y_{t+k|t}$ and r are the predicted output variables and the output set-points, respectively. The output set-points can now be reformulated depending on the desired speeds by the driver or $r = r(t)$. The weighting matrices of $Q = Q' \geq 0$ and $R = R' > 0$ are applied for the predicted outputs and the input increments.

For MPC regulator tracking setpoints, the steady-state variables are kept equal to the target set-points when there are no disturbances and constraints. Formula (31) is the one that we apply for the remainder of this chapter to test the ability of MPC to control the HEV velocities.

In this research, we assume that the MPC outputs horizon length is set equal to the inputs control horizon, i.e., $N_u = N_y = N_p$ (equal to the predictive lengths). The quadratic objective junction $J(U, x(t))$ in equation (4.3) is minimized over a vector N_p future prediction inputs starting from the state $x(t)$.

For the MPC with hard constraints, by substituting $x_{t+N_p|t} = A^{N_p}x(t) + \sum_{k=0}^{N_p-1} A^k B u_{t+N_p-1-k}$, equation (31) can be rewritten as a function of the current state $x(t)$ and the current setpoints $r(t)$:

$$\Psi\left(x(t), r(t)\right) = \frac{1}{2}x^t(t)Yx(t) + \min_U\left\{\frac{1}{2}U'HU + x'(t)r(t)FU\right\}, \tag{32}$$

subject to the hard combined constraints of $GU \le W + Ex(t)$, where the column vector $U \triangleq \left[\Delta u_t, \ldots, \Delta u_{t+N_p-1}\right]' \in \Delta\mathcal{U}$ is the MPC optimization vector; $H = H' > 0$, and then, H, F, Y G, W and E are proceeding matrices obtained from Q, R and $x(t)$, $r(t)$ in equation (4.1). Because that we use only the optimizer U, other terms involving Y are normally removed from equation (32). Therefore, the optimal problem in (4.4) will be a purely quadratic formula and depending on only the current state variables $x(t)$, and the current set-points $r(t)$. Implementation of MPC always requires the real-time solution of each quadratic program for each discrete time steps.

In fact, the system may have always both input and output constraints. Difficulties will be arised due to the inability to respond to all output constraints because of the already input constraints. Since MPC is applied for the real-time implementation, any infeasible solution of the optimal control problems cannot be tolerated. Basically if the input constraints are set from the system physical limits and usually considered as the hard/unchanged constraints. At the same time, if the system outputs constraints are the measured velocities and the unmeasured torques which are not so much strictly imposed and can be violated somewhat during the movement of the vehicles. In order to guarantee the system stability if some outputs may violate the constraints, equation (32) can be transformed to some other soften constraints.

$$\begin{aligned}&\Psi\left(x(t), r(t)\right) = \frac{1}{2}x^t(t)Yx(t) + \min_U\left\{\frac{1}{2}U'HU + x'(t)r(t)FU + \frac{1}{2}\varepsilon_i'(t)\Lambda\varepsilon_i(t)\right\},\\ &\text{subject to } \varepsilon_i(t) = \left[\varepsilon_y; \varepsilon_u\right], y_{\min} - \varepsilon_y \le y_{t+k|t} \le y_{\max} + \varepsilon_y \text{ and } u_{\min} - \varepsilon_y \le u_{t+k|t} \le u_{\max} + \varepsilon_u\end{aligned} \tag{33}$$

The new weighting items, $\varepsilon_i(t)$, are added into the MPC soften objective function: $\Lambda > 0$ (generally some small values) become the weighting factors, $\varepsilon_i(t)$ are represent the violation penalty terms ($\varepsilon_i(t) \ge 0$) for the scheme objective function. These values will keep the output violations at low levels until the constrained solution can be appeared. Further reference of the MPC's subject to these soften state constraints can be read from reference [16].

http://dx.doi.org/10.5772/61415

In order to increase the ability of MPC to get on-line solutions for some critical times, some of the output set-points can be temporally deleted since if some output set-points are omitted, the system will become looser and then, the possibility that MPC can find some solutions will increase. Temporally omitting of some output set-points can also be performed by putting some zeros into the weighting matrix Q in equation (33). The robustness of MPC scheme can be also increased if some output set-points become relaxed into regions rather than in some hard values. If the system output constraints are set into output regions, the MPC scheme will need to change slightly because the set-points $r(t)$ in equation (33) now turn regions. In this formula, output regions are defined by the minimum and maximum limits in a desired output range. The maximum value is the upper limit and the minimum value is the lower limit, $y_{lower} \le y_{t+k|t} \le y_{upper}$. From this range, a modified MPC objective function for the output regions is developed as:

$$\begin{aligned} &\min_{U \triangleq \left\{\Delta u_1, \ldots, \Delta u_{1+N_u-1}\right\}} \left\{ J(U, x(t)) = \sum_{k=0}^{N_y-1} \left[z'_{t+k|t} Q z_{t+k|t} + \Delta u'_{t+k} R \Delta u_{t+k} \right] \right\}, \\ &\text{where } z_{t+k|t} \ge 0; z_{t+k\}t} = y_{t+k|t} - y_{upper} \text{ for } y_{t+k|t} > y_{upper}; \\ &z_{t+k|t} = y_{lower} - y_{t+k|t} \text{ for } y_{t+k|t} < y_{lower}; z_{t+k|t} = 0 \text{ for } y_{lower} \le y_{t+k|t} \le y_{upper} \end{aligned} \tag{34}$$

When the system outputs are still laid inside the desired regions, there is no control action being taken, due to none of the control outputs are violated ($z_{t+k|t}=0$). But if some outputs come to violate the desired regions, MPC regulator in equation (34) will activate the objective function, find out optimal inputs action to push the outputs back to the desired regions. Further MPC developments with output constraints deletion and output regions can be referred in reference [17]. We now illustrate the robustness of MPC for soften output constraints and the constraint regions in the following part.

4.1. MPC control application for EM2

The MPC control for EM2 is used for driving the HEVs at the slow speed (less 50 km/h). In this moment the friction clutch is open and both ICE and EM1 are turned off. The dynamic equation of the system in this case is formulated in equation (3.24). The MPC objective function applied in this system is developed in equations (4.3), (4.5), and (4.6). The discrete time interval of all simulations is set at 0.01 sec.

Parameters used for the EM2 are: torsional rigidity, k_θ=1158; motor constants, k_{E2}=k_{T2}=10; motor inertia, J_2=1; load inertia, J_3=2; gear ratio, i=2.34; motor damping, $k_{\beta 2}$=0.5; load damping, $k_{\beta 3}$=12; armature resistance, R_{I2}=5.

The input constraints in this example are set as follows: control constraints for the DC input voltage for the vehicle is $|V_2| \le 300V$; $\Delta u(t) \le$inf, or in this case, there is no need to set the input limit increments on $\Delta u(t)$. The physical output constraints are set for the motor shaft with an allowable shear stress (carbon steel), τ=25 (MPa or N/mm²). The constraint for the output

torque on shaft2 is $|T| = \tau\pi\frac{d^3}{16}$, where $d = 0.05m$ is the output shaft diameter of the motor. Then, the output torque constraint will be $|T_2| \leq 455Nm$.

The MPC parameters will be selected as the horizon prediction length, $N_u = N_y = N_p = 5$, the weighting matrices, $Q = \begin{bmatrix} 10 & 0 \\ 0 & 10 \end{bmatrix}$ and $R = [1]$. Figure 11 shows the MPC performance with the input voltage, the output speed, and torque.

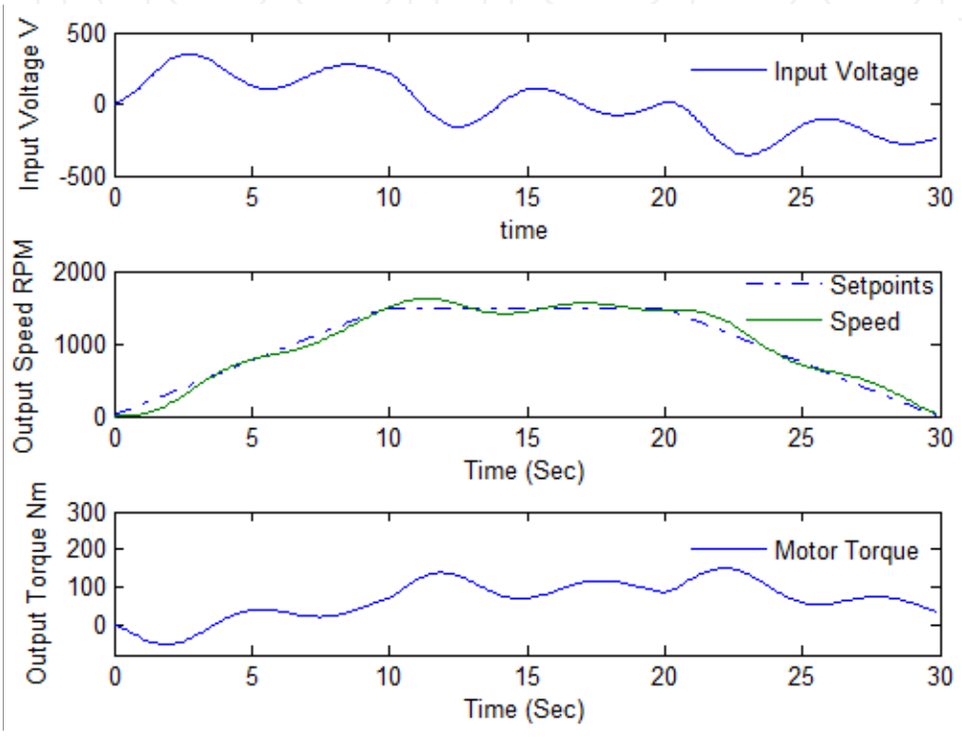

Figure 11. MPC performance with $N_p = 5$ and $Q = 10R$.

Because the MPC performance is highly relying on the selection of the values in weighting matrices Q and R. If we choose that Q is much bigger than R ($Q \gg R$), then, the voltage input control increment $\Delta u(t)$ will become much bigger than the output penalty in $(y(t) - r)$ as indicated in the MPC objective function in (6.3). The controller will drive the vehicle to track the output set-points very fast, but in return, the vehicle will need very much great energy for input torques as illustrated in Figure 12.

In the simulation, the horizon prediction is chosen as $N_u = N_y = N_p = 5$ and the values for weighting matrices are selected as $Q = \begin{bmatrix} 100 & 0 \\ 0 & 100 \end{bmatrix}$ and $R = [1]$:

The MPC horizon length of prediction is highly influenced by its performance. The system will become looser if a longer prediction horizon is selected and the MPC will achieve better performance since the system becomes more flexible and then it is easier to find out better

http://dx.doi.org/10.5772/61415

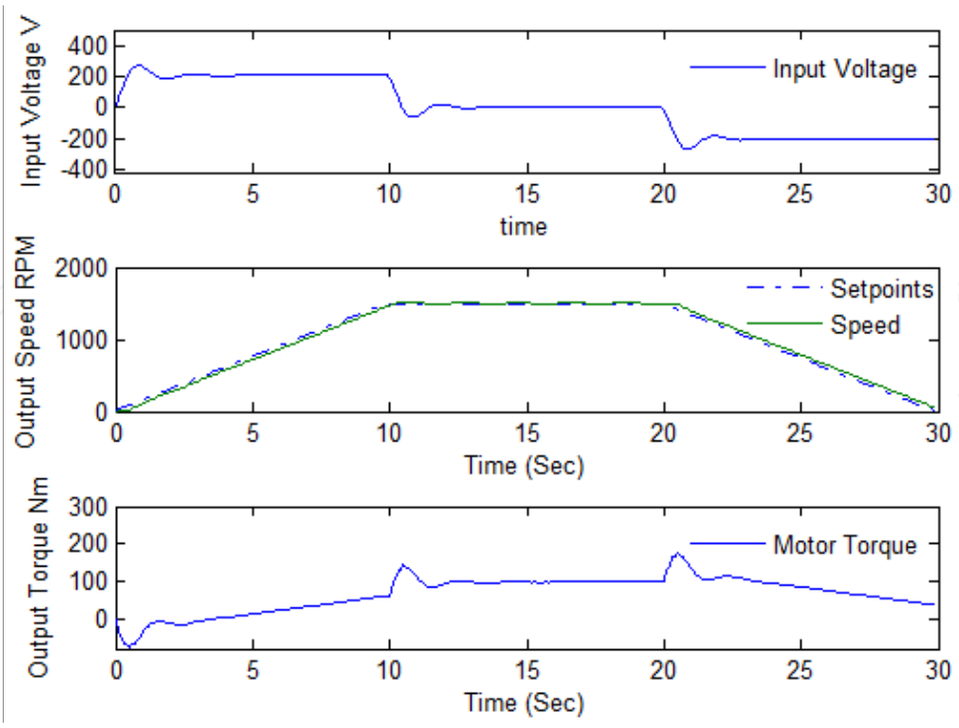

Figure 12. MPC performance with $N_p=5$ and $Q=100R$.

solutions. However with the longer prediction, the burden of the computer calculation will exponentially rise up and the time for calculating the optimal actions will depend on the ability of the CPU and the speeds of the communication protocols. In the next simulation, we run the MPC controller with a very shorter horizon length of $N_u=N_y=N_p=2$; and with medium values of $Q=\begin{bmatrix}50 & 0\\ 0 & 50\end{bmatrix}$ and $R=[1]$. Result of this simulation is shown in Figure 13.

As shown in Figure 13, for very short horizon length prediction of $N_p=2$. The MPC controller performance becomes worse since the system cannot properly track the output set-points. And then, compared to the next simulation with a longer horizon length prediction, the MPC will achieve a much better performance.

The horizon length prediction is now chosen even longer for $N_u=N_y=N_p=10$ and for the same values of weighting $Q=\begin{bmatrix}50 & 0\\ 0 & 50\end{bmatrix}$ and $R=[1]$, the performance of this controller is shown in Figure 14.

The MPC scheme with longer prediction length in Figure 14 indicates better performance compared to that in Figure 13. However in this simulation, the much higher input energy is required for the input DC voltages.

A fact is that if we impose an input constraint for voltage of $|V_2|\leq 300V$ and because that the DC motor basically runs in only positive voltage or $0\leq V_2\leq 300V$. The braking and the recharged system will be started if we want to slow down the vehicle speed. In the next example, we will

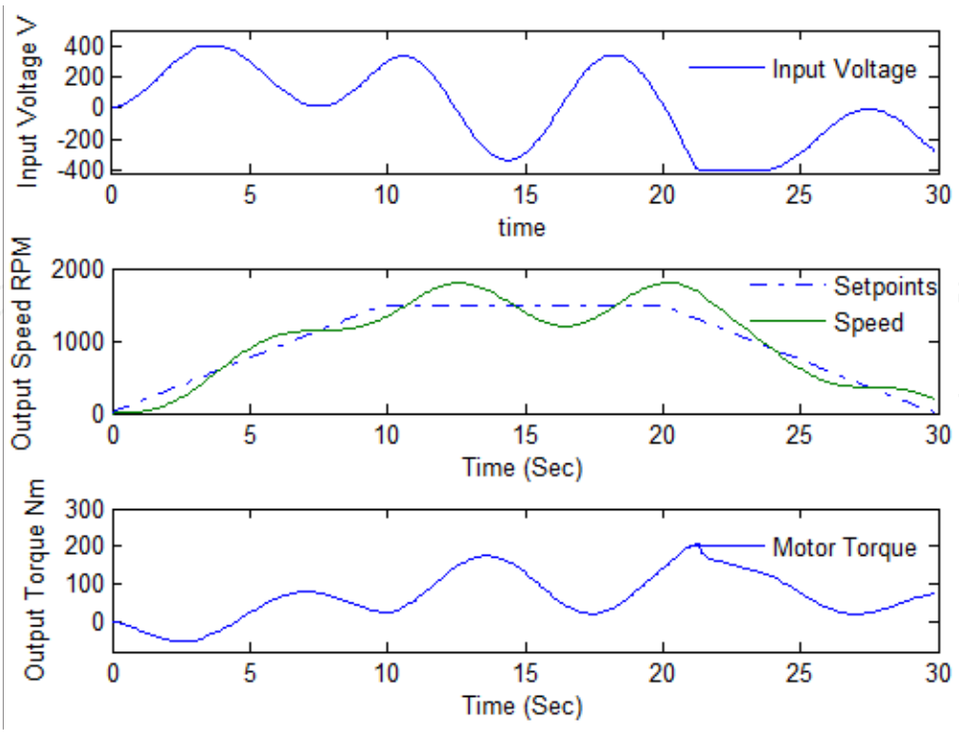

Figure 13. MPC performance with horizon length $N_p = 2$ and $Q = 50R$.

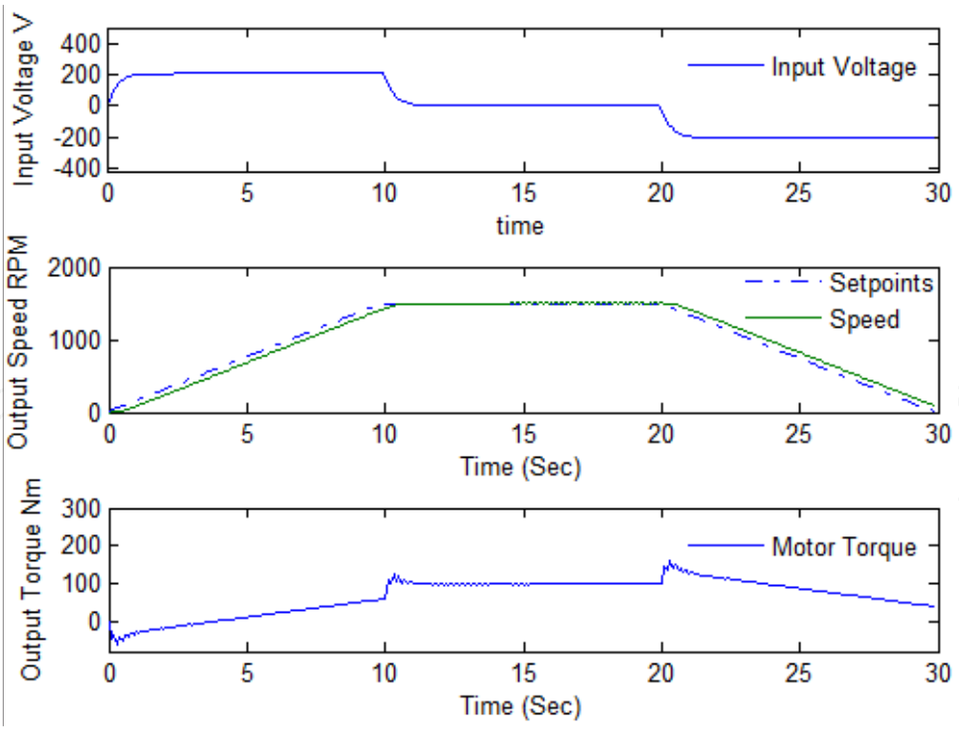

Figure 14. MPC performance with horizon length $N_p = 10$ and $Q = 50R$.

http://dx.doi.org/10.5772/61415

set the input voltage for the DC motor on only positive values of $0 \le V_2 \le 300V$. This simulation allows for the regenerative braking option when we start braking to slow down the speed. The performance of this simulation is shown in Figure 15 for the horizon length of $N_u = N_y = N_p = 5$ and high weighting values of $Q = \begin{bmatrix} 1000 & 0 \\ 0 & 1000 \end{bmatrix}$ and small weighting value of $R = [1]$.

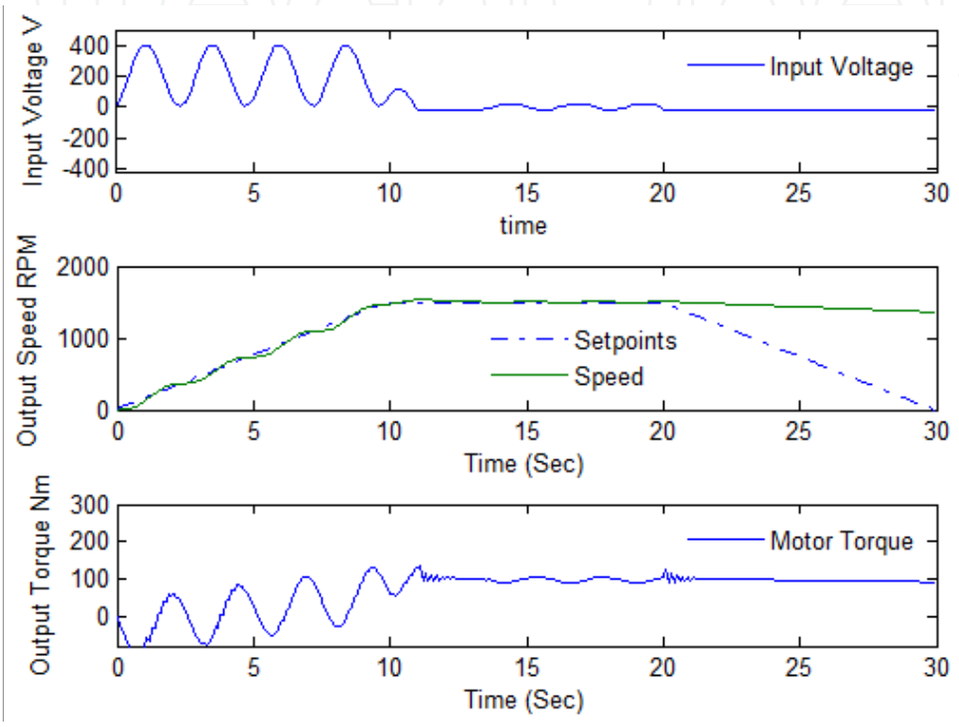

Figure 15. MPC performance with $0 \le V_2 \le 300V$, $N_p = 5$ and $Q = 1000R$.

Simulations for the MPC performance with the motor EM2 have been conducted with the change of parameters in the weighting matrices, horizon prediction length, and with the input voltage constraints. For the next part, we will investigate the MPC controller for the ICE and the EM1 to track the desired speed set-points applied for the vehicle high speeds (above 50 km/h) and investigate how to synchronize the velocities of these two parts with the friction clutch engagement.

4.2. MPC performance for ICE and EM1

If the speed of the vehicle exceeds 50 km/h, EM1 will start and activate the ICE to drive the vehicle. Depending on the needed requirements of the speeds and the torques, this hybrid vehicle can configure to operate only the ICE or all ICE, and/or EM1 and/or EM2. For the starting time, the friction clutch is still open and the dynamic formula for the vehicle in the ICE and EM1 is indicated as in equation (27).

The example parameters used for the EM1 are: motor constants, k_{E2}=k_{T2}=15; motor inertia, J_1=1; motor damping, $k_{\beta 1}$=0.5; armature resistance, R_{I1}=7; compensation factor, ς=0.5. The system is discretized at a time interval of 0.01 sec. The air drag resistance torque at ω_3=2000 rpm is chosen as M_{v0}=30 Nm.

The physical input constraints for this vehicle are set for the DC voltage in range of $|V_1| \leq 48V$; The input increment constraint is $\Delta u(t) \leq 180V$ / sec. The output constraint of torque for the shaft1 is set for $|T_1| \leq 628Nm$.

The MPC parameters are chosen for the horizon length prediction of N_u=N_y=N_p=5, the weighting values for the matrices of $Q=\begin{bmatrix}10 & 0\\ 0 & 10\end{bmatrix}$ and $R=\begin{bmatrix}1 & 0\\ 0 & 1\end{bmatrix}$. Figure 16 shows the MPC performance at the starting time.

From Figure 16, after a certain delay time of 1 second, the ICE is fully started and after about 2.4 seconds the peed of ICE has reached the set-point of 2000 rpm and operate stably at a power of 6 kW, generating an output torque of 30 Nm (at this moment, the friction clutch is still open).

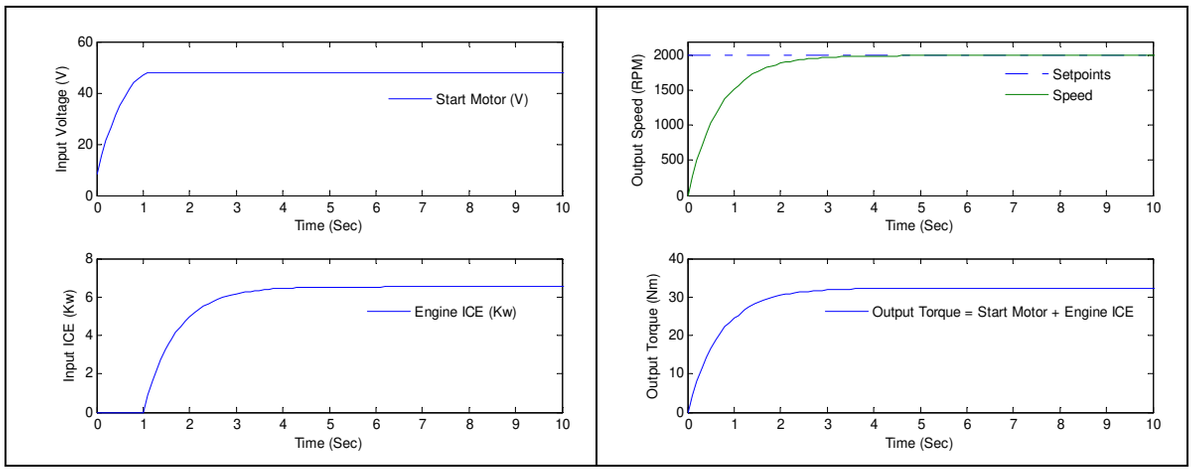

Figure 16. MPC performance at the starting time.

Next, we run the hybrid vehicle with this EM1 and ICE to track the speed set-points and test for the clutch engagement. It is assumed that if the motor EM2 operating at more than 1500 rpm, the motor EM1 will start and activate the ICE to engage to the system. Regarding the improvement of the driving comfort and the reduction of jerk, the clutch engagement will be taken place for only when $\omega_1 \geq \omega_2$ or ω_1=1.05.ω_2 or the EM1 and ICE must track the EM2 at 5% positive offset. The MPC objective function in (4.3) is now changed from setpoints $r(t)$ to track $\omega_2(t)$ with 5% positive offset. Results of the simulation are shown in Figure 17. The system reaches the setpoint and ready for the clutch engagement after 2.5 seconds.

In the simulation in Figure 17, we operate both motor EM1 and the ICE to track motor EM2 and we can observe that after around 2 sec, the speed of the left hand side clutch disk has exceeded more than 5% of the speed on the right hand side disk and ready for the clutch

http://dx.doi.org/10.5772/61415

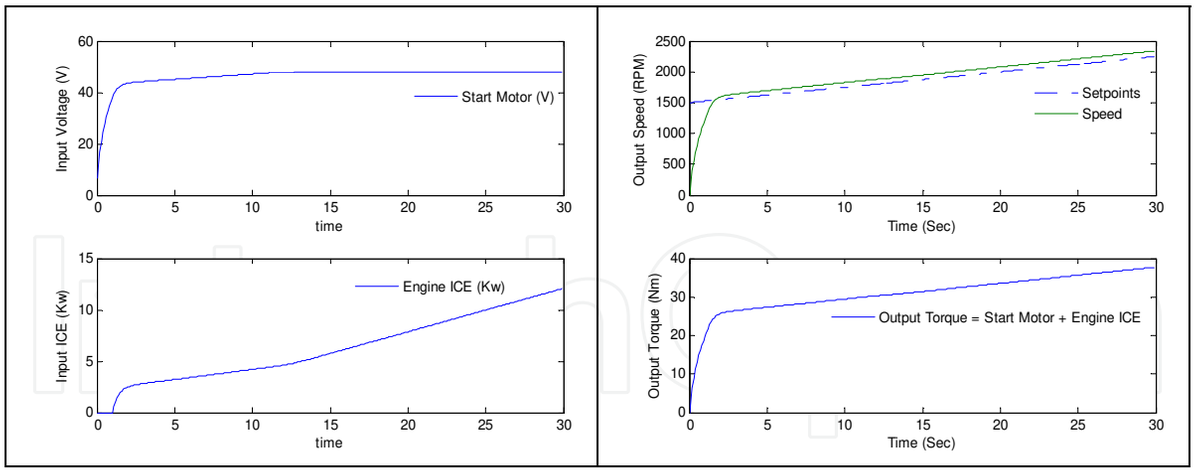

Figure 17. MPC controller for tracking setpoint with both EM1 and ICE.

engaged. However, the motor EM1 functions only for as the ICE starter and once the ICE is fully run, the EM1 can be turned on to as an electrical generator to charge the batteries. In the next example, we will turn off the motor EM1 and use only the ICE to track the speed of the motor EM2. The MPC objective function becomes now similar to the example that we have simulated in Figure 17. Results of the performance are illustrated in Figure 18. The vehicle will reach the speed set-point and ready for the clutch engaged after around 4.4 sec.

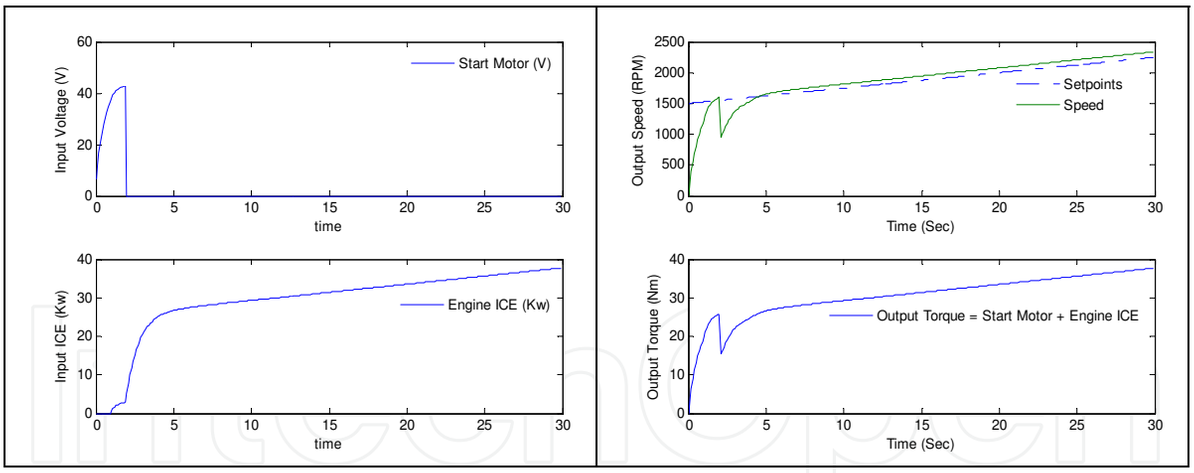

Figure 18. MPC controller for tracking setpoint with only ICE.

How to control the ω_1 rapidly tracking $\omega_2 + 5\%$ by MPC controller is still a big challenge. Next, we test a new MPC controller using the soften output constraints when we consider the output tracking setpoints as in (4.5) with some additional penalty terms added into the MPC objective function, $J_{Soften} = J_{Hard} + \Lambda\varepsilon_i^2(t)$. Results of the simulation are shown in Figure 19.

In Figure 19, additional penalty terms ε_i and a new weighting matrix Λ can be regulated independently together with values of matrices Q and R to obtain some good soften constraints

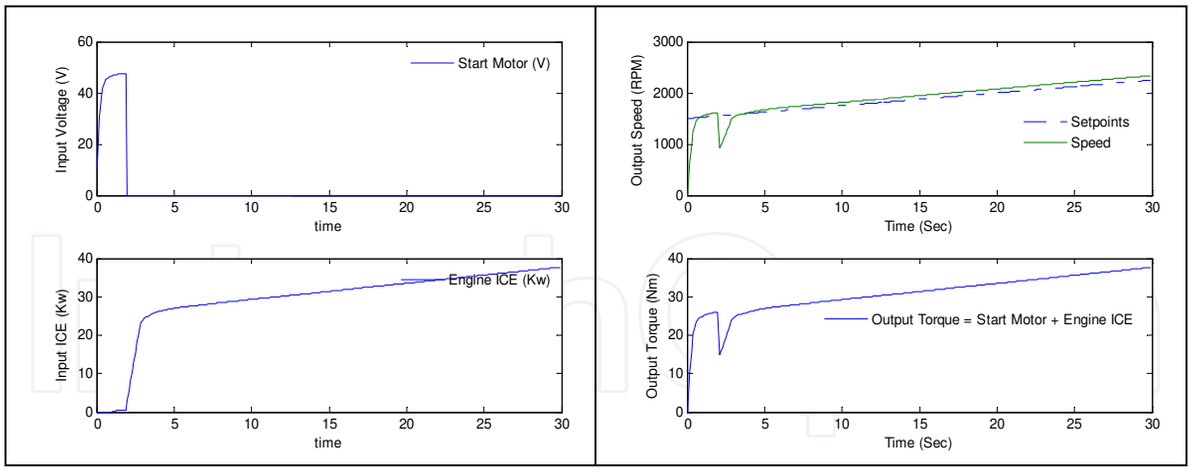

Figure 19. Soften output constraints for tracking set-point with only ICE.

controller performance. The MPC controller becomes looser, more flexible with more regulated parameters. The new system reaches the set-point faster and ready for the clutch engagement after only about 3.4 sec.

5. Conclusions

As a main type of hybrid vehicle, HEVs have achieved better fuel economy and performances. Modern HEV can also improve the efficiency by using the energy from braking and bring other potential environmental benefits. The electric vehicle charging stations can use the low cost and green energy sources from GRID, wind and solar. Due to rapid development in battery technology, the normal electric recharging time has been reducing significantly from 8 h to less than 2 h. The fast recharging time for a modern electric vehicle is now reduced to less than 10 min. Hybrid electric vehicle technology has been applied now not only for the passenger cars but also for all heavy buses and trucks.

The new modeling and control strategy for HEV using MPC has been developed. Reason for using this new control strategy is that, firstly, MPC can solve the optimization problems online with both linear and nonlinear systems, and secondly, MPC can deal with the constraints in the open-loop optimal control problems. MPC can find real-time solution for general constrained nonlinear models over a finite predictive horizon length. Therefore, the performances of the hybrid vehicle can be significantly improved.

The new HEV dynamic modeling equations allow having better studied views for the acceleration of HEVs and the jerk reduction during the transitional engagement period. Examples show that MPC controllers can control the speeds very well to track to any desired speeds. Examples also indicate that the MPC controller can be able to achieve fast and smooth engagement of clutch. The MPC performance can also be considerably improved when we select some appropriate prediction lengths and the values of the weighting values. MPC controller can provide online the optimal control actions subject to the input voltages and

http://dx.doi.org/10.5772/61415

output torque constraints. The MPC modified schemes can improve the system performance robustness if some output torque constraints can be softened or turned into the constrained regions.

Acknowledgements

The authors would like to thank the Tallinn University of Technology (TTU) for supporting the preparation of this research article.

Author details

Vu Trieu Minh*, Alina Sivitski, Mart Tamre and Igor Penkov

*Address all correspondence to: trieu.vu@ttu.ee

Department of Mechatronics, Faculty of Mechanical Engineering, Tallinn University of Technology, Tallinn, Estonia

References

[1] Langari R.; Won J.S., A driving situation awareness-based energy management strategy for parallel hybrid vehicles, Proc. Future Transportation Technol Conf, California, 2003; 1; 95-102.

[2] Graaf van der R; Daniel B; Spijker E., Integration of drive system, subsystems and auxiliary systems of a flywheel hybrid driveline with respect to design aspects and fuel economy, Hybridantriebe: Tagung Garching, VDI-Verlag, Düsseldorf, 1999, 1, 459-67.

[3] Lukic S.M.; Emadi A., Effects of drivetrain hybridization on fuel economy and dynamic performance of parallel hybrid electric vehicles, IEEE Transactions on Vehicular Technology, 2004, 53 (2), 385-89.

[4] Jalil N.; Kheir N.A.; Salman, M., A rule-based energy management strategy for a series hybrid vehicle, Proc. American Control Conference, Albuquerque, 1997, 1, 689-93.

[5] Schouten, N. J.; Salman, M. A.; Kheir, N. A., Fuzzy logic control for parallel hybrid vehicles, IEEE Transactions on Control Systems Technology, 2002, 10 (3), 460-68.

[6] Kim, T.S; Manzie, C.; Sharma, R., Model predictive control of velocity and torque split in a parallel hybrid vehicle, Proc. IEEE International Conference on Systems, San Antonio, 2009, 13 (2), 2014 - 19.

[7] Paganelli, G.; Delprat, S.; Guerra, T.M.; Rimaux, J.; Santin, J.J., Equivalent consumption minimization strategy for parallel hybrid powertrains, Proc. IEEE Vehicular Technology Conference, Columbus, 2002, 4, 2076-81.

[8] Sciarretta, A.; Back, M.; Guzzella, L., Optimal control of parallel hybrid electric vehicles, IEEE Transactions on Control Systems Technology, 2004, 12 (3), 352–63.

[9] Qin, S.J.; Badgwell, T.J., An overview of industrial model predictive control technology, AIChE Symposium Series, 1997, 316, 232 56.

[10] Findeisen, R.; Diehl, Z.; Nagy, F.; Allgower, H.; Schloder, J., Computational feasibility and performance of nonlinear model predictive control schemes, Proc. International Conference on Chemical Process Control, Arizona, 2001, 1, 454-60.

[11] Rawlings, J., Tutorial overview of model predictive control, *IEEE Contr. Syst. Mag.*, 2000, 20 (3), 38-62.

[12] Morari, M.;Lee, J., Model predictive control: Past, present and future, Comput. Chem. Eng., 1999, 23 (4), 667-82.

[13] Mayne, D.; Michalska, H., Robust receding horizon control of constrained nonlinear systems, Proc. IEEE C*onference on Decision and Control*, 1993, 38, 1623-33.

[14] Chen, H.; F. Allgower, Nonlinear Model Predictive Control Schemes with Guaranteed Stability, Kluwer Academic Publishers, New York, 1998, 465-94.

[15] Minh, V.T.; Afzulpurkar, N., A comparative study on computational schemes for nonlinear model predictive control, Asian Journal of Control, 2006, 8 (4), 324-31.

[16] Minh, V.T.; Afzulpurkar, N., Robust model predictive control for input saturated and soften state constraints, Asian Journal of Control, 2005, 7 (3), 323-29.

[17] Minh, V.T.; Afzulpurkar, N., Robustness of model predictive control for ill-conditioned distillation process, International Journal of Developments in Chemical Engineering and Mineral Processing, 2005, 13 (3/4), 331-16.

[18] Karden, E.; Ploumen, S.; Fricke, B.; Miller, T.; Snyder, K., Energy storage devices for future hybrid electric vehicles, Journal of Power Sources, 2007, 168, 2-11.

[19] Fredriksson, J.; Egbert, B., Nonlinear control applied to gearshifting in automated manual transmissions, Proc. IEEE Conference on Decision and Control, Sydney, 2000, 1, 444-49.

[20] Powell, B. K.; Bailey, K. E.; Cikanek, S. R., Dynamic modelling and control of hybrid electric vehicle powertrain systems, IEEE *Control Systems Magazine*, 1998, 18 (5), 17-33.

[21] Minh, V.T.; Afzulpurkar, N.; Muhamad, W., Fault detection and control of process systems, Mathematical Problems in Engineering, 2007, Article ID 80321, 20 pages.

http://dx.doi.org/10.5772/61415

[22] Guzzella, L.; Sciarretta, A., Vehicle Propulsion Systems, Introduction to Modeling and Optimization; Springer, Zurich, 2007.

[23] Chan, C. C., The state of the art of electric, hybrid, and fuel cell vehicles, Proceedings of the IEEE, 2007, 95 (4), 704-18.

[24] Miller, J. M., Propulsion Systems for Hybrid Vehicles. IET. 1st edn., London, 2008.

[25] Sciaretta, A.; Guzzella, L., Control of hybrid electric vehicles, IEEE Control Systems Magazine, 2007, 27 (2), 60-70.

[26] Ripaccioli, G.; Bernardini, D.; Di Cairano, S.; Bemporad, A.; Kolmanovsky, V., A stochastic model predictive control approach for series hybrid electric vehicle power management, Proc. American Control Conference, Baltimore, 2010, 1, 5844–49.

[27] Desai, C.; Williamson, S., Comparative study of hybrid electric vehicle control strategies for improved drivetrain efficiency analysis, Electrical Pwoer & Energy Conference, Montreal, 2009, 1, 1-6.

IntechOpen

IntechOpen

IntechOpen